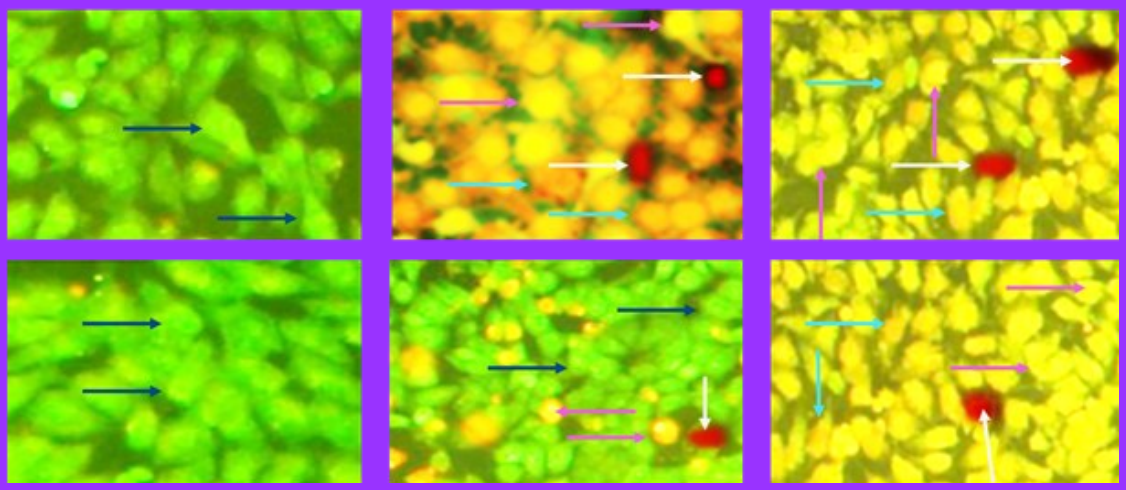

BJP

Bangladesh Journal of Pharmacology

Research Article

Tangeretin suppresses HER2-driven breast cancer via PI3K/AKT/mTOR inhibition and caspase-dependent apoptosis

A Journal of the Bangladesh Pharmacological Society (BDPS)
Journal homepage: www.bdpsjournal.org; www.banglajol.info
Abstracted/indexed in Academic Search Complete, Agroforestry Abstracts, Asia Journals Online, Bangladesh Journals Online, Biological Abstracts, BIOSIS Previews, CAB Abstracts, Current Abstracts, Directory of Open Access Journals, EMBASE/Excerpta Medica, Global Health, Google Scholar, HINARI (WHO), International Pharmaceutical Abstracts, Open J-gate, Science Citation Index Expanded, SCOPUS and Social Sciences Citation Index
Bangladesh J Pharmacol 2026; 21: 1-10
ISSN: 1991-0088

Tangeretin suppresses HER2-driven breast cancer via PI3K/AKT/mTOR inhibition and caspase-dependent apoptosis

Jaggareddygari Shruthi Reddy and Puligilla Shankaraiah

Department of Pharmacology, Chaitanya Deemed to be University, Kishanpura, Hanamkonda, Warangal-506001, India.

Article Info

Received: 20 November 2025
Accepted: 26 December 2025
Available Online: 2 March 2026

DOI: 10.3329/bjp.v21i1.85717

Cite this article:
Reddy JS, Shankaraiah P. Tangeretin suppresses HER2-driven breast cancer via PI3K/AKT/mTOR inhibition and caspase-dependent apoptosis. Bangladesh J Pharmacol. 2026; 21: 1-10.

Abstract

Tangeretin, a citrus-derived polymethoxylated flavone, exhibits potent and selective anti-cancer activity against HER2-positive breast cancer. It demonstrated cytotoxicity in SKBR3 cells (IC_{50} = 19.5 ± 1.7 µM) and MCF-7 cells (IC_{50} = 36.2 ± 2.4 µM), while sparing non-tumorigenic MCF-10A cells (>90% viability; IC_{50} = 327.5 ± 18.2 µM). Tangeretin markedly reduced clonogenic survival (51.4 ± 3.1 colonies in SKBR3; 78.1 ± 3.7 in MCF-7) and induced pronounced apoptosis, as evidenced by late apoptotic staining (50.6 ± 2.3%), DNA laddering, and strong activation of caspase-3/7 (3.4 ± 0.1-fold) and caspase-9 (2.9 ± 0.1-fold). Flow cytometry revealed significant G_2/M phase arrest in SKBR3 cells (38.9 ± 2.0%). Mechanistically, tangeretin suppressed AKT kinase activity (0.4 ± 0.04-fold), comparable to MK-2206 (0.3 ± 0.0-fold), and reduced the expression of phosphorylated HER2 (p-HER2), p-PI3K, p-AKT, p-mTOR, p-p70S6K, and cyclin D1. These findings establish tangeretin as a selective HER2-targeted anti-cancer candidate that acts through dual inhibition of the PI3K/AKT/mTOR pathway and induction of mitochondrial apoptosis.

Introduction

Breast cancer is the most frequently diagnosed malignancy and a leading cause of cancer-related mortality among women, accounting for over 2.3 million new cases and nearly 685,000 deaths worldwide (Sung et al., 2021). Human epidermal growth factor receptor 2-positive (HER2+) breast cancer represents approximately 15–20% of cases and is driven by the amplification or overexpression of the ERBB2 oncogene (Slamon et al., 2001; Loibl and Gianni, 2017). This subtype is clinically aggressive, characterized by rapid disease progression, high metastatic potential, and poorer survival outcomes (Moja et al., 2012).

Although HER2-targeted therapies such as trastuzumab, pertuzumab, lapatinib, and T-DM1 have significantly improved patient outcomes, intrinsic and acquired resistance remains a major clinical challenge (Rimawi et al., 2015; Vu and Claret, 2012).

The phosphoinositide 3-kinase (PI3K)/AKT/mammalian target of rapamycin (mTOR) signaling pathway is a critical downstream effector of HER2 signaling. Its hyperactivation promotes uncontrolled proliferation, survival, metabolic reprogramming, angiogenesis, and drug resistance (Miller et al., 2011; Mayer and Arteaga, 2016). Aberrations in this pathway—including PIK3CA mutations, PTEN loss, and elevated AKT/mTOR activity are strongly associated with aggressive tumor biology and poor responses to HER2-targeted therapies (Loibl et al., 2016). Therefore, compounds capable of

simultaneously suppressing multiple nodes within the PI3K/AKT/mTOR axis are being actively investigated as promising therapeutic strategies for cancer treatment.

Plant-derived flavonoids have garnered significant attention due to their pleiotropic anti-cancer effects and low toxicity toward normal tissues (Panche et al., 2016). Tangeretin, a polymethoxylated flavone predominantly found in *Citrus reticulata* and *C. sinensis*, exhibits a wide range of pharmacological properties, including anti-inflammatory, antioxidant, cardioprotective, neuroprotective, and anti-cancer effects (Li et al., 2022; Guo et al., 2014). It has demonstrated broad-spectrum anti-cancer activity against breast, colon, liver, lung, prostate, and glioma malignancies (Miyata et al., 2018; Chen et al., 2020). Mechanistically, tangeretin modulates key cancer -associated pathways such as PI3K/AKT, MAPK, STAT3, NF-κB, and Wnt/β-catenin, resulting in apoptosis, cell cycle arrest, and reduced metastatic potential (Fang et al., 2016; Lai et al., 2011). In breast cancer models, it downregulates cyclin D1, inhibits Bcl-2, activates caspases, and enhances sensitivity to chemotherapeutic agents such as doxorubicin and paclitaxel (Braga et al., 2021; Lai et al., 2007). Additionally, tangeretin has shown potential in overcoming drug resistance by modulating multidrug resistance proteins and suppressing cancer stem cell characteristics (Zhang et al., 2020). However, its precise mechanistic effects on HER2 -positive breast cancer remain unclear. Given the central role of PI3K/AKT/mTOR signaling in HER2-driven oncogenesis and therapeutic resistance, evaluating the inhibitory potential of tangeretin on this axis represents a rational therapeutic approach.

This study investigates the antiproliferative and pro-apoptotic effects of tangeretin on HER2-positive breast cancer cells, emphasizing the suppression of the PI3K/AKT/mTOR pathway and the induction of caspase-dependent apoptosis. These mechanistic insights highlight tangeretin's potential as a phytotherapeutic agent or adjuvant treatment for HER2-driven breast cancer.

Materials and Methods

Cell culture

HER2-positive SKBR3, ER-positive MCF-7, and non-tumorigenic MCF-10A human mammary epithelial cells (ATCC origin; procured from CCMB, Hyderabad) were used in this study. SKBR3 cells were maintained in McCoy's 5A medium supplemented with 10% fetal bovine serum (FBS) and 1% penicillin/streptomycin. MCF-7 cells were cultured in high-glucose DMEM containing 10% FBS and 1% penicillin–streptomycin. MCF-10A cells were grown in DMEM/F12 (1:1) supplemented with 5% horse serum, EGF (20 ng/mL), hydrocortisone (0.5 µg/mL), cholera toxin (100 ng/mL), insulin (10 µg/mL), and 1% penicillin–streptomycin. All cultures were maintained in T-75 flasks at 37°C in a humidified 5% CO_2 incubator. Media were refreshed every 48–72 hours, and cells were subcultured at 70–80% confluence using 0.25% trypsin–EDTA. Experiments were performed using cells between passages 5 and 20 to ensure phenotypic stability.

Morphological analysis

Morphological changes associated with cytotoxicity and apoptosis were examined following treatment with tangeretin at IC_{50} concentrations. Cells (2 x 10^5/well) were seeded into 6-well plates, allowed to adhere for 24 hours, and then exposed to tangeretin for an additional 24 hours. Doxorubicin (1 µM) and untreated cells served as positive and negative controls, respectively. Cellular morphology was observed using an inverted

Box 1: MTT assay

Principle

The cytotoxicity of the test samples was evaluated using the MTT assay, a standard colorimetric method for quantifying viable, metabolically active cells.

Requirements

96-Well plate, Antibiotic antimycotic cocktail, Dulbecco's Modified Eagles Medium (DMEM)-high glucose, ER-positive MCF-7, Formazan, HER2-positive SKBR3, Isopropanol, Microplate reader (Tecan Infinite F500, Switzerland), PBS, MTT, Tangeretin, Trypsin

Procedure

Step 1: Cells were seeded into 96-well plates at a density of 5 × 10^3 cells/well in 100 µL of DMEM and allowed to adhere overnight

Step 2: After cell adherence, the respective treatment concentrations of tangeretin (1–50 µM; ≤0.1% DMSO) were added, and the cells were incubated for 24 hours

Step 3: Following the treatment period, the culture medium was gently aspirated, and the wells were washed with 200 µL phosphate-buffered saline (PBS) to remove any residual compounds

Step 4: Subsequently, 50 µL of MTT solution (5 mg/mL prepared in PBS) was added to each well, and the plate was incubated for 3 hours to allow metabolically active cells to form insoluble formazan crystals

Step 5: After incubation, the MTT solution was carefully removed, and 200 µL of DMSO was added to each well to dissolve the formed formazan crystals

Step 6: The plate was incubated for 2 hours to ensure complete solubilization. The absorbance of each well was measured at 570 nm using a microplate reader. Cell viability (%) was calculated relative to that of the untreated control cells

Reference

Riss et al., 2016

phase-contrast microscope (Olympus, Japan) at 20x magnification. Representative images were captured to assess hallmark apoptotic features, including cell rounding, detachment, membrane blebbing, cytoplasmic shrinkage, and nuclear condensation. Pronounced apoptotic changes were observed in SKBR3 and MCF-7 cells, whereas MCF-10A cells exhibited minimal alterations.

Colony formation assay

The long-term anti-proliferative effect of tangeretin was evaluated using a clonogenic assay, which measures the ability of single cells to form macroscopic colonies (Brix et al., 2020). SKBR3 and MCF-7 cells were seeded in 6-well plates at a density of 500 cells/well in 2 mL of complete medium and allowed to adhere overnight. The cells were then treated with tangeretin at their IC_{50} concentrations in serum-free medium (≤0.1% DMSO). Doxorubicin (10 µM) served as a positive control. After 24 hours, the treatment medium was replaced with fresh complete medium, and the cultures were maintained for 14 days at 37°C in 5% CO_2, with medium renewal every 3–4 days. Colonies were fixed with 4% paraformaldehyde for 15 minutes, stained with 0.5% crystal violet for 30 min, washed, and air-dried. Colonies containing ≥50 cells were counted manually, and plating efficiency and relative clonogenic survival were calculated relative to untreated controls.

Evaluation of apoptosis

Apoptosis induction by tangeretin was evaluated using complementary morphological, biochemical, and molecular assays after 24 hours of treatment of SKBR3 and MCF-7 cells with their respective IC_{50} concentrations. Doxorubicin (10 µM) and untreated cultures served as positive and negative controls, respectively.

EB/AO dual fluorescence staining

Apoptotic nuclear morphology was assessed using ethidium bromide/acridine orange (EB/AO) staining, a widely used and cost-effective fluorescence-based method for distinguishing viable, apoptotic, and necrotic cells (Liu and Liu, 2015). Cells (2×10^5 cells/well) were seeded in 6-well plates and incubated overnight before treatment with tangeretin for 24 hours. Harvested cells were washed twice with PBS, resuspended in 25 µL of PBS, and mixed with an equal volume of EB/AO solution (100 µg/mL). The stained cells were immediately examined under a fluorescence microscope (Olympus). Live cells exhibited uniform green fluorescence; early apoptotic cells showed bright green nuclei with chromatin condensation, while late apoptotic or necrotic cells displayed orange-red fluorescence with nuclear fragmentation.

DNA fragmentation assay

Internucleosomal DNA fragmentation was assessed using the classical method described by Wyllie, which detects apoptotic DNA laddering as a hallmark of programmed cell death (Zhao et al., 2019). SKBR3 cells were treated with tangeretin at its IC_{50} concentration for 24 hours, with doxorubicin (10 µM) serving as a refer-ence control. Cells were lysed on ice for 30 min in lysis buffer (10 mM Tris-HCl, pH 7.4; 10 mM EDTA; 0.5% triton X-100) and centrifuged at 12,000 x g for 15 min at 4°C. The supernatants were treated with RNase A (50 µg/mL, 37°C, 30 min) and Proteinase K (100 µg/mL, 55°C, 1 hour). DNA was precipitated with isopropanol and 3 M sodium acetate, washed, air-dried, and resus-pended in TE buffer. Samples were separated on 1.5% agarose gels stained with ethidium bromide, and apop-totic ladder patterns were visualized under UV illumi-nation.

Caspase-3/7 activity assay

Executioner caspase activation was quantified using the luminescent Caspase-Glo® 3/7 assay (Promega, USA), a sensitive and homogeneous method for monitoring caspase activity in 96-well plates (Niles et al., 2016). SKBR3 cells were seeded in white 96-well plates at a density of 1×10^4 cells/well and incubated overnight. Cells were then treated with tangeretin at IC_{50} concentrations for 24 hours, with doxorubicin (10 µM) serving as a positive control. After treatment, 100 µL of Caspase -Glo® reagent was added to each well, mixed gently, and incubated for 30 min at room temperature in the dark. Luminescence was measured using a BioTek luminometer, based on a chemiluminescent reaction with a peak emission at approximately 560 nm. Caspase -3/7 activity was expressed as relative luminescence intensity compared to untreated controls.

Caspase-9 activity assay

Mitochondria-mediated apoptosis was evaluated using a fluorometric caspase-9 activity assay kit (Abcam, UK), which detects the cleavage of an LEHD-conjugated fluorescent substrate as an indicator of initiator caspase activation (Riss et al., 2016). SKBR3 cells were treated with tangeretin at their IC_{50} concentrations for 24 hours, with doxorubicin (10 µM) serving as the positive con-trol. Cells were harvested, lysed on ice, and centrifuged at 12,000 x g for 10 min at 4°C. The supernatants were then incubated with 50 µL LEHD-AFC substrate at 37°C for 1 hour. Fluorescence was measured at excitation/emission wavelengths of 400/505 nm. Caspase-9 activi-ty was expressed as the fold change relative to untrea-ted controls.

Cell cycle analysis by flow cytometry

Cell cycle distribution was analyzed following propidium iodide staining and DNA content assessment by flow cytometry, according to established protocols for cell cycle analysis (Pozarowski and Darzynkiewicz, 2004). SKBR3 cells were seeded in 6-well plates (2×10^5

cells/well) and incubated overnight, then treated with tangeretin at IC_{50} concentrations for 24 hours. Doxorubicin (10 µM) and untreated cultures served as positive and negative controls, respectively. After treatment, both floating and adherent cells were collected, washed with cold PBS, and fixed in 70% ethanol at −20 °C for at least 12 hours. The fixed cells were washed, treated with RNase A (100 µg/mL, 37°C, 30 min), and stained with PI (50 µg/mL) for 30 min in the dark. A minimum of 10,000 events per sample were acquired using a BD FACSCalibur (488 nm laser). Data were analyzed using FlowJo (v5.2) and the Watson Pragmatic model to determine the distributions of G_0/G_1, S, and G_2/M phases. The phase percentages of treated and control groups were compared to evaluate tangeretin-induced cell cycle arrest.

AKT kinase activity assay

AKT kinase activity was quantified in SKBR3 cells using a non-radioactive ELISA-based AKT kinase assay kit (Abcam, UK), which is conceptually similar to established immunoprecipitation kinase assays employing GSK-3 fusion protein substrates (Maadi et al., 2014). Cells were seeded in 6-well plates and grown to 70–80% confluence before treatment with tangeretin at its IC_{50} concentration for 24 hours. MK-2206 (5 µM) and untreated cells served as positive and negative controls, respectively. Following treatment, cells were washed with cold PBS and lysed in kinase extraction buffer supplemented with protease and phosphatase inhibitors. Total AKT was immunoprecipitated using AKT antibody–conjugated beads and incubated with the GSK-3α/β fusion protein substrate in the presence of ATP at 30°C. Phosphorylation of GSK-3α/β (Ser21/9) was detected using a phospho-specific primary antibody, followed by an HRP-conjugated secondary antibody and TMB substrate. Absorbance was measured at 450 nm using a BioTek reader. Reduced absorbance indicates decreased AKT kinase activity. Assays were performed in triplicate and normalized to untreated controls.

Western blot analysis of PI3K/AKT/mTOR pathway proteins

Western blotting was performed to evaluate the modulation of HER2-driven PI3K/AKT/mTOR signaling. SKBR3 cells were seeded in 6-well plates (5×10^5 cells/well), allowed to adhere overnight, and treated with tangeretin at its IC_{50} concentration for 24 hours. DMSO-treated cultures served as negative controls, while MK-2206 (2 µM) was used as a pathway-specific positive control. After treatment, the cells were washed with ice-cold PBS and lysed in RIPA buffer (pH 7.4) supplemented with protease and phosphatase inhibitors. The lysates were incubated on ice for 30 min and centrifuged at 14,000 x g for 15 min at 4°C. Protein concentration was determined using a BCA assay. Equal amounts of protein (30-40 µg) were resolved on 10% SDS-PAGE gels and transferred onto PVDF membranes. Membranes were blocked with 5% BSA in TBS-T for 1 hour and incubated overnight at 4°C with primary antibodies (1:1000; Cell Signaling Technology) against p-HER2 (Tyr1248), p-PI3K (Tyr458), p-AKT (Ser473), p-mTOR (Ser2448), p-p70S6K (Thr389), and cyclin D1. After washing, membranes were incubated with HRP-conjugated secondary antibodies (1:3000) for 1 hour at room temperature. Protein bands were detected using an ECL substrate (Bio-Rad) and imaged with a Chemi-Doc™ MP system. β-Actin served as the loading control. Band intensities were quantified using ImageJ, a validated platform for densitometric analysis of scientific images (Schneider et al., 2012), and normalized to β-actin.

Statistical analysis

All experiments were performed in triplicate, and the data are presented as the mean ± standard deviation (SD). Statistical analyses were conducted using GraphPad Prism 6.0. Group comparisons were performed using one-way ANOVA followed by Tukey's post-hoc test. For pairwise comparisons, an unpaired two-tailed Student's t-test was used. Differences were considered statistically significant at $p<0.05$.

Results

Cytotoxic effect

The cytotoxicity of tangeretin was evaluated in SKBR3, MCF-7, and MCF-10A cells using the MTT assay. Tangeretin reduced the viability of SKBR3 and MCF-7 cells in a concentration-dependent manner, while exerting minimal effects on MCF-10A cell viability (Figure 1).

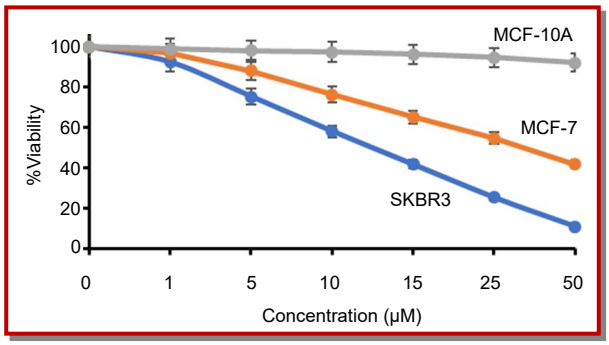

Figure 1: Effect of tangeretin on the viability of SKBR3, MCF-7, and MCF-10A cells. Cells were exposed to tangeretin (1–50 µM) for 48 hours, and cell viability was quantified using the MTT assay. Data are presented as mean ± SD (n = 3)

SKBR3 cells exhibited the highest sensitivity to tangeretin, with an IC_{50} of 19.5 ± 1.6 µM, and viability decrea-sed to 10.8 ± 2.6% at 50 µM (Table I). Doxorubicin (10 µM) reduced SKBR3 viability to 28.7 ± 3.0% (IC_{50}: 12.8 ± 1.2 µM). In MCF-7 cells, tangeretin showed moderate

Table I

Effect of tangeretin on cell viability

Cell line	IC_{50} of tangeretin (μM)	IC_{50} of doxorubicin (μM)
SKBR3	19.5 ± 1.6	12.8 ± 1.2
MCF-7	36.2 ± 2.4	15.6 ± 1.7
MCF-10A	327.5 ± 18.2	295.4 ± 15.8

Values are mean ± SD; n=3

cytotoxicity (IC_{50}: 36.2 ± 2.4 μM), resulting in 41.6 ± 2.4% viability at 50 μM, whereas doxorubicin exhibited grea-ter potency (IC_{50}: 15.6 ± 1.7 μM). Conversely, tangeretin displayed minimal cytotoxicity in MCF-10A cells, main-taining over 90% viability across all tested concentra-tions, with an IC_{50} of 327.5 ± 18.2 μM. Doxorubicin reduced MCF-10A viability to 60.4 ± 2.3% at 10 μM (IC_{50}: 295.4 ± 15.8 μM).

Morphological analysis of tangeretin-treated cells

Morphological changes induced by tangeretin were examined in SKBR3, MCF-7, and MCF-10A cells at their respective IC_{50} concen-trations. Untreated SKBR3 and MCF-7 cells exhibited epithelial-like morpho-logies, whereas MCF-10A cells formed uniform cobblestone-like monolayers (Figure 2A). Upon tangeretin exposure, SKBR3 cells showed marked cyto-plasmic shrinkage, membrane blebbing, and detachment from the substrate surface. SKBR3 cells treated with doxo-rubicin also displayed apoptotic changes, although the extent of these alterations differed. Tangeretin-treated MCF-7 cells demonstrated reduced cell density, loss of intercellular contacts, and formation of apoptotic bodies. In contrast, MCF-10A cells maintained normal morphological features with minimal structural alterations following tangeretin treatment.

Effect on clonogenic potential of breast cancer cells

The effect of tangeretin on long-term proliferative capacity was evaluated using a colony formation assay in SKBR3 (HER2-positive) and MCF-7 (ER-positive) cells. As shown in Figure 2B-C, untreated SKBR3 and MCF-7 cells formed abundant colonies, with mean colony numbers of 92.5 ± 4.2 and 100.2 ± 5.1, respectively. Treatment with tangeretin at IC_{50} concentrations significantly reduced the clonogenic survival rates of both cell lines. In SKBR3 cells, the colony number decreased to 51.4 ± 3.1 ($p<0.01$ vs. control), whereas in MCF-7 cells, it decreased to 78.1 ± 3.7 ($p < 0.05$ vs. control). Doxorubicin (10 μM) further

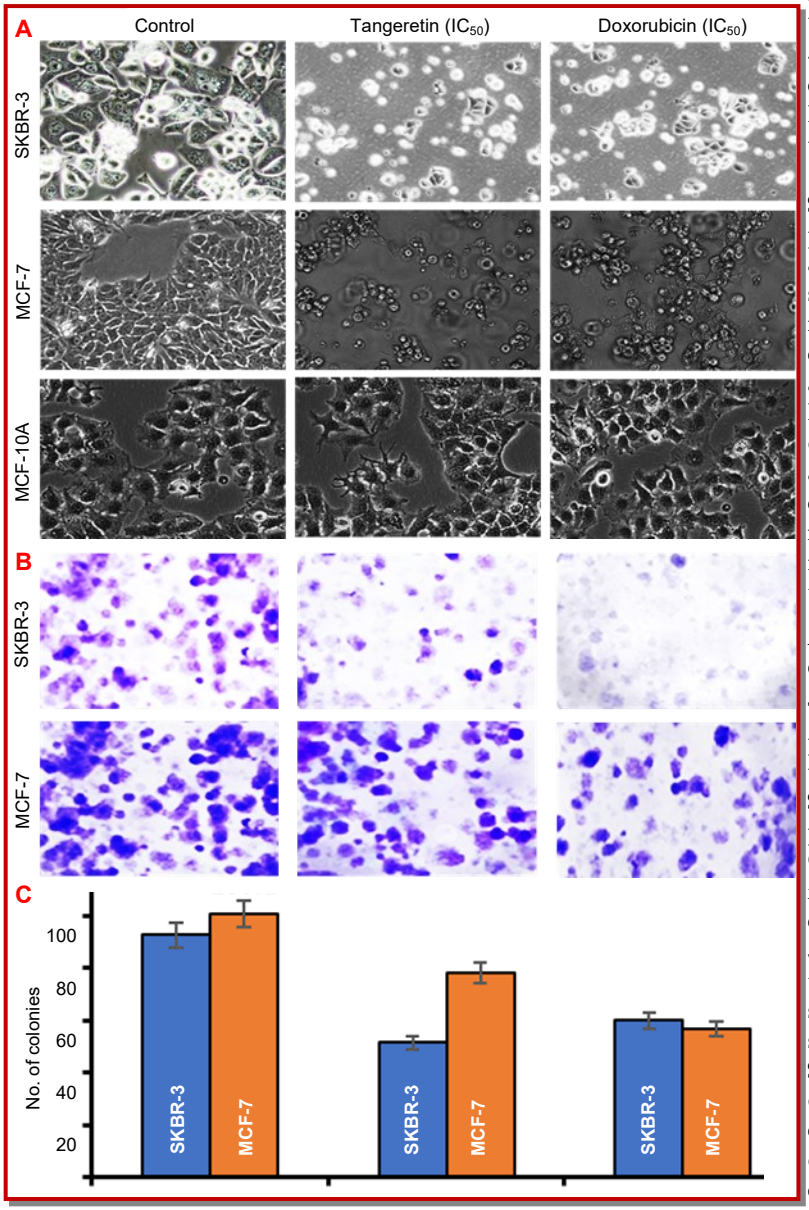

Figure 2: Morphological changes were observed in SKBR3, MCF-7, and MCF-10A cells after 24-hours of treatment with tangeretin at their respective IC_{50} concentrations: 19.5 μM for SKBR3, 36.2 μM for MCF-7, and 327.5 μM for MCF-10A. Images were captured using phase-contrast microscopy at a magnification of 20x (A). Effect of tangeretin and doxorubicin on the clonogenic survival of SKBR3 and MCF-7 cells; Representative images of crystal violet-stained colonies in SKBR3 and MCF-7 cells treated with vehicle (control), tangeretin at their respective IC_{50} concentrations: 19.5 μM for SKBR3 and 36.2 μM for MCF-7, or doxorubicin for 14 days (B); Quantitative colony counts expressed as mean ± SD (n = 3) (C)

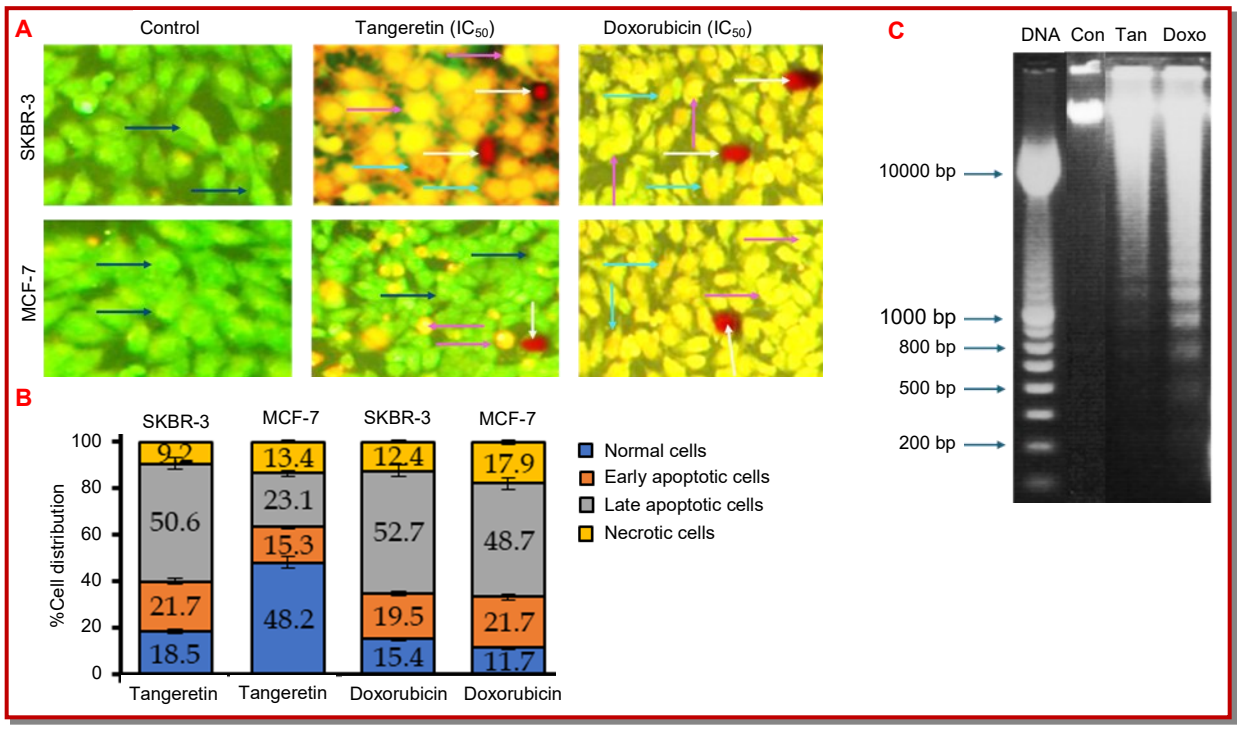

Figure 3: Representative fluorescence micrographs showing EB/AO-stained SKBR3 and MCF-7 cells after tangeretin and doxorubicin treatment. Arrows indicate viable (blue), early apoptotic (pink), late apoptotic (white), and necrotic (light blue) cells (A); Quantitative bar graph representing the percentage distribution of normal, early apoptotic, late apoptotic, and necrotic cells in each treatment group (B). Data are expressed as mean ± SD (n = 3); Representative image of DNA fragmentation analysis of SKBR3 cells. Cells treated with tangeretin (IC_{50}) and doxorubicin (10 µM) were subjected to agarose gel electrophoresis (C). DNA: DNA ladder; Tan: Tangeretin; Doxo: doxorubicin

suppressed colony formation, yielding 47.8 ± 2.6 colonies in SKBR3 and 52.4 ± 2.9 colonies in MCF-7 cells, respectively.

Evaluation of apoptosis by EB/AO dual fluorescence staining

Apoptotic induction by tangeretin was evaluated in SKBR3 and MCF-7 cells using EB/AO dual-fluorescence staining after 24 hours of exposure to IC_{50} concen-trations. As shown in Figure 3A-B, tangeretin treatment increased the proportion of late apoptotic cells in both cell lines, with SKBR3 exhibiting 50.6 ± 2.3% and MCF-7 exhibiting 23.1 ± 2.7% late apoptosis, respectively. Correspondingly, the percentage of viable cells decrea-sed to 18.5 ± 1.4% in SKBR3 cells and 48.2 ± 1.9% in MCF-7 cells. The necrotic population remained low in both cell lines, with 9.2 ± 0.9% in SKBR3 cells and 13.4 ± 1.4% in MCF-7 cells. In comparison, doxorubicin treat-ment resulted in 52.7 ± 3.9% late apoptotic cells in SKBR3 and 48.7 ± 2.9% in MCF-7, accompanied by reductions in viable cell numbers. The necrosis percentages were slightly higher in the doxorubicin-treated groups than in the tangeretin-treated groups.

DNA fragmentation assay

Internucleosomal DNA fragmentation was evaluated in SKBR3 cells treated with tangeretin at its IC_{50} concentra-tion for 24 hours. As shown in Figure 3C, tangeretin-treated cells exhibited a distinct laddering pattern consisting of discrete oligonucleosomal fragments approximately 180–200 bp. A similar laddering profile was observed in the doxorubicin-treated control. Untreated control cells (data not shown) displayed intact genomic DNA without fragmentation. The fragmentation patterns in both tangeretin- and doxorubicin-treated samples were comparable in terms of band clarity and distribution.

Evaluation of caspase-3/7 and caspase-9 activities

Caspase activation following tangeretin treatment was quantified in SKBR3 and MCF-7 breast cancer cells. Tangeretin increased both caspase-3/7 and caspase-9 activities in a cell line-dependent manner (Figure 4A). In SKBR3 cells, tangeretin induced a 3.4 ± 0.18-fold increase in caspase-3/7 activity and a 2.9 ± 0.16-fold increase in caspase-9 activity relative to the untreated control. Doxorubicin produced comparable increases of 3.8 ± 0.22-fold and 3.1 ± 0.20-fold, respectively. In MCF-7 cells, tangeretin resulted in a 2.3 ± 0.15-fold increase in caspase-3/7 activity and a 1.8 ± 0.1-fold increase in caspase-9 activity. Doxorubicin elicited stronger activation in MCF-7 cells, yielding 2.9 ± 0.19-fold and 2.3 ± 0.17-fold increases in caspase-3/7 and caspase-9 activities, respectively.

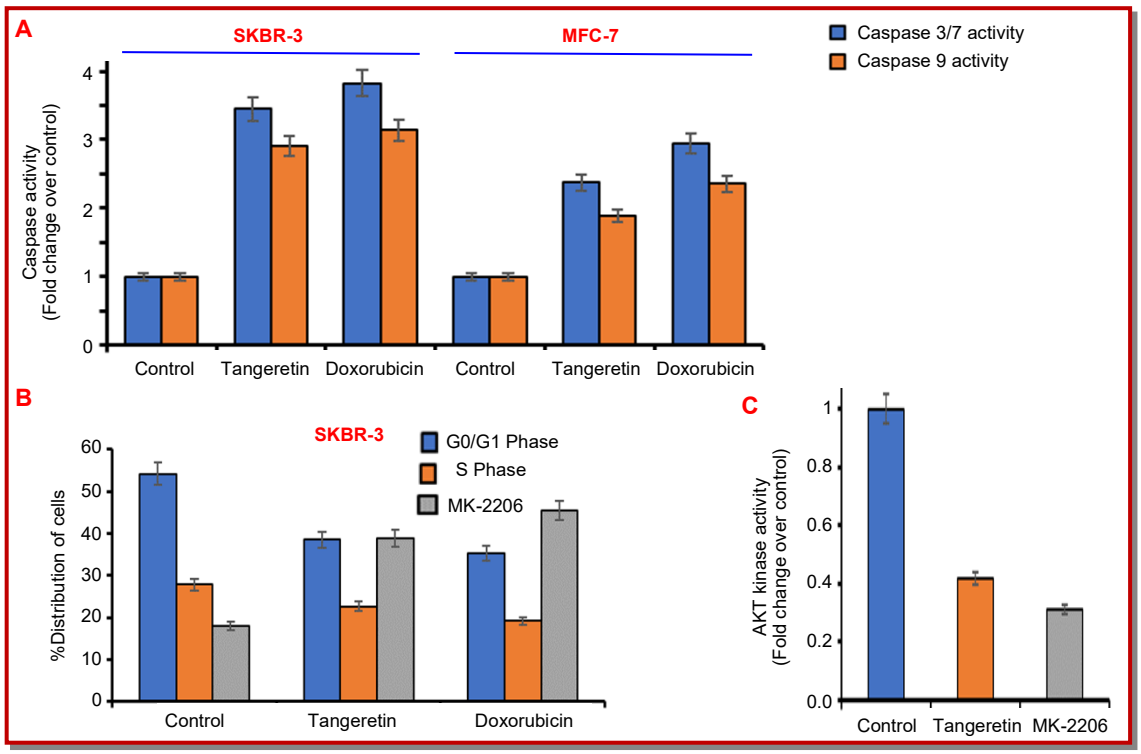

Figure 4: Quantitative analysis of caspase-3/7 and caspase-9 activities in SKBR3 and MCF-7 breast cancer cells after 24-hours treatment with tangeretin at their respective IC_{50} concentrations: 19.5 µM for SKBR3 and 36.2 µM for MCF-7 and doxorubicin (10 µM). Untreated cells were used as controls (control). Caspase-3/7 and caspase-9 activities were measured using luminescent and fluorometric assay kits, respectively, and expressed as fold-change over the control (A); Effects of tangeretin and doxorubicin on cell cycle distribution in SKBR-3 breast cancer cells. The cells were treated with tangeretin at its IC_{50} concentration of 19.5 µM or doxorubicin (10 µM) for 24 hours and stained with propidium iodide for flow cytometry. The percentage distribution of cells in the G_0/G_1, S, and G_2/M phases was determined using FlowJo software (B). Effect of tangeretin and MK-2206 on AKT kinase activity in SKBR-3 breast cancer cells. The cells were treated with tangeretin at its IC_{50} concentration of 19.5 µM or MK-2206 (5 µM) for 24 hours. AKT activity was measured using a cell-based ELISA to quantify GSK-3α/β phosphorylation at Ser21/9; The results are expressed as fold changes relative to those of the untreated control (C). Data are the mean ± SD of three independent experiments

Cell cycle analysis by flow cytometry

The effect of tangeretin on cell cycle progression was evaluated in SKBR3 cells after 24 hours of treatment at the IC_{50} concentration. As shown in Figure 4B, tangeretin-treated cells exhibited an increased proportion of cells in the G_2/M phase (38.9 ± 2.0%) compared to untreated controls (18.0 ± 1.5%).

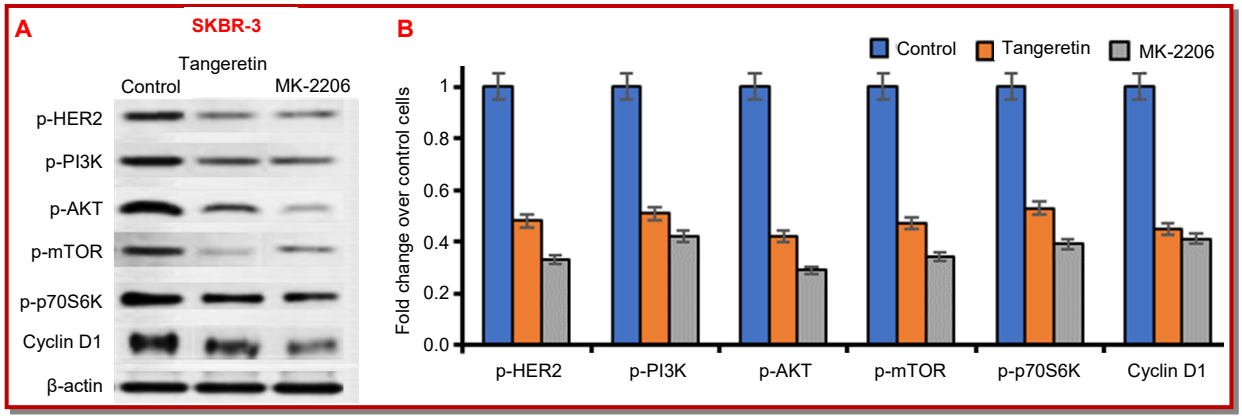

Figure 5: Representative western blot images showing the expression of phosphorylated HER2 (p-HER2), PI3K (p-PI3K), AKT (p-AKT), mTOR (p-mTOR), p70S6K (p-p70S6K), and cyclin D1 in SKBR3 cells treated with vehicle control (DMSO), tangeretin at its IC_{50} concentration of 19.5 µM or MK-2206 (2 µM) for 24 hours. β-actin was used as the internal loading control (A); Densitometric quantification of the protein bands in the panel, expressed as fold change relative to control and normalized to β-actin (B). The data represent the mean ± SD of three independent experiments (n = 3). $p<0.05$, vs. control; statistical analysis was performed using one-way ANOVA followed by Tukey's post-hoc test

Correspondingly, there was a decrease in the G_0/G_1 phase population (38.5 ± 1.9% vs. 54.2 ± 2.1% in controls) and in the S phase (22.6 ± 1.1% vs. 27.8 ± 1.3%). Doxorubicin-treated cells exhibited a greater accumulation in the G_2/M phase (45.4 ± 2.4%), accompanied by further reductions in the G_0/G_1 (35.4 ± 1.7%) and S-phase (19.2 ± 1.2%) fractions.

Evaluation of AKT kinase activity

AKT kinase activity was quantified in SKBR3 cells after 24 hours of treatment with tangeretin at its IC50 concentration of 19.5 μM. As shown in Figure 4C, untreated control cells exhibited normalized AKT activity (1.0 ± 0.06-fold). Tangeretin-treated cells showed a significant reduction in AKT kinase activity, decreasing to 0.4 ± 0.04-fold. The positive control, MK-2206, further reduced activity to 0.3 ± 0.03-fold. These data indicate that tangeretin reduced the phosphorylation of the AKT substrate GSK-3α/β under the tested conditions.

Western blot analysis of the PI3K/AKT/mTOR signaling pathway

The effect of tangeretin on the PI3K/AKT/mTOR signaling pathway was evaluated in SKBR3 cells using western blotting. As shown in Figure 5A-B, tangeretin treatment for 24 hours reduced the phosphorylation of several key signaling proteins. Compared to the untreated control, p-HER2 decreased to 0.4 ± 0.0-fold, p -PI3K to 0.5 ± 0.0-fold, and p-AKT to 0.4 ± 0.1-fold. Additionally, p-p70S6K and cyclin D1 levels were reduced to 0.5 ± 0.1 and 0.4 ± 0.0-fold, respectively. Cells treated with the AKT inhibitor MK-2206 (2 μM) showed further reductions in these phosphoproteins, with fold changes ranging from 0.2 to 0.4, depending on the target.

Discussion

Tangeretin exhibited a robust and selective anti-cancer profile against HER2-overexpressing SKBR3 cells, with comparatively moderate effects on ER-positive MCF-7 cells and negligible toxicity on non-tumorigenic MCF-10A cells. This selectivity is consistent with the unique dependence of HER2-driven tumors on hyperactivated PI3K/AKT/mTOR signaling, a pathway extensively reported to be vulnerable to flavonoid-mediated modulation (Huang et al., 2018; Lee and Kim, 2020; Singh et al., 2021). The preferential cytotoxicity observed in SKBR3 cells indicates that tangeretin disrupts HER2-linked survival mechanisms more effectively than in luminal ER-restricted phenotypes, which rely on distinct endocrine-regulated signaling pathways and often exhibit flavonoid resistance (Wang et al., 2017). Morphological analyses supported the cytotoxicity findings, revealing classical apoptotic hallmarks—including cytoplasmic shrinkage, membrane blebbing, detachment, and apoptotic body formation—in tangeretin-treated SKBR3 and MCF-7 cells. These morphological changes were more pronounced in SKBR3 cells, underscoring their heightened susceptibility to tangeretin-induced apoptosis. In contrast, MCF-10A cells largely retained their normal epithelial morphology, reinforcing the compound's selective action toward malignant phenotypes. This observation aligns with earlier studies showing that polymethoxylated flavones selectively perturb oncogenic kinases in malignant cells without compromising normal cell integrity (Chen et al., 2019). Tangeretin also significantly impaired long-term proliferative capacity, as evidenced by reduced clonogenic survival in SKBR3 and MCF-7 cells. The stronger suppression in SKBR3 cells further confirmed HER2-dependent vulnerability. Although doxorubicin exhibited greater potency, tangeretin demonstrated comparable inhibition of colony formation with a potentially improved safety margin, highlighting its potential as a natural, pathway-directed antiproliferative agent.

Apoptosis-specific assays provided convergent mechanistic evidence supporting this conclusion. EB/AO fluorescence staining revealed a substantially higher proportion of late apoptotic cells in SKBR3 cells compared to MCF-7 cells, confirming differential apoptotic signaling intensity. DNA fragmentation studies further validated the activation of caspase-dependent nucleases, with SKBR3 cells exhibiting pronounced internucleosomal laddering comparable to that induced by doxorubicin, indicating that tangeretin triggers classical programmed cell death. The low necrotic fraction across treatments suggests that tangeretin induces controlled apoptosis rather than nonspecific necrosis, a clinically favorable attribute. Caspase profiling supported activation of the intrinsic mitochondrial apoptotic pathway. Tangeretin markedly stimulated both caspase -9 and caspase-3/7, with significantly stronger activation observed in SKBR3 cells. Given that HER2-positive cancers maintain survival through AKT-mediated stabilization of mitochondrial membranes, the enhanced caspase-9 response likely reflects disruption of upstream PI3K/AKT signaling. This response parallels earlier findings linking flavones to mitochondrial outer membrane permeabilization and cytochrome c release (Zhao et al., 2020). Robust executioner caspase activation reinforces efficient propagation of apoptotic signals to the terminal death machinery. Flow cytometric analysis revealed that tangeretin induced a distinct G_2/M phase arrest in SKBR3 cells, consistent with its interference in mitotic progression.

Previous study has shown that flavonoids can activate Chk1/Chk2 kinases or inhibit cyclin B1/cdc2 function, leading to delayed mitotic entry (Park et al., 2016). The observed G_2/M arrest likely contributes to the initiation of apoptosis, acting as a pre-apoptotic checkpoint consistent with caspase activation and DNA fragmentation. Mechanistically, the most compelling evidence

comes from the AKT kinase assay and western blot analysis, which demonstrate that tangeretin exerts multi-level suppression of the PI3K/AKT/mTOR pathway, a key survival signaling axis in HER2-positive breast cancers. Tangeretin inhibited AKT activity to a

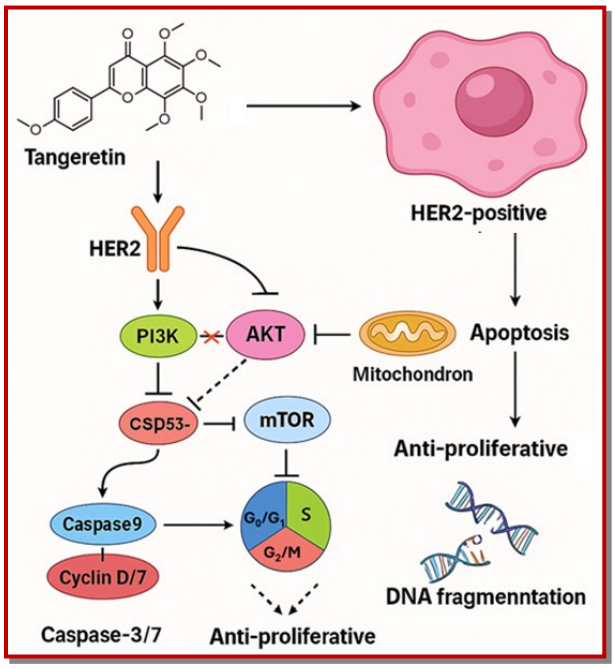

Figure 6: Proposed mechanistic pathway of tangeretin in HER2 -positive breast cancer cells: Tangeretin inhibits HER2-mediated activation of the PI3K/AKT/mTOR axis, leading to the suppression of downstream effectors, including Cyclin D1 and p70S6K. AKT inhibition promotes mitochondrial dysfunction, caspase-9 and caspase-3/7 activation, DNA fragmentation, and apoptosis. Concurrently, the downregulation of mTOR and cyclin D1 contributes to G_2/M arrest and antiproliferative effects. Overall, tangeretin induced selective apoptotic and cytostatic responses in HER2-overexpressing breast cancer cells

similar extent as MK-2206, a clinically validated AKT inhibitor, indicating that it functions as a potent natural kinase modulator. Western blotting confirmed the significant downregulation of phosphorylated HER2 (p-HER2), PI3K (p-PI3K), AKT (p-AKT), mTOR (p-mTOR), and p70S6K (p-p70S6K), and D1. These alterations are mechanistically consistent with a reduced proliferative drive, induction of G_2/M arrest, and activation of mitochondrial apoptosis pathways. Notably, suppression of cyclin D1 was directly associated with the cell cycle perturbations observed in SKBR3 cells, reinforcing the coherence of the mechanistic findings.

These integrated mechanistic insights are summarized in Figure 6, which illustrates the proposed pharmacological mechanism: tangeretin suppresses HER2-mediated activation of the PI3K/AKT/mTOR signaling pathway, induces G_2/M cell cycle arrest, activates intrinsic caspase pathways, promotes DNA fragmentation, and ultimately triggers selective apoptosis in HER2-overexpressing breast cancer cells. Collectively, these findings position tangeretin as a promising natural therapeutic candidate capable of targeting HER2-driven breast cancer through coordinated inhibition of survival signaling networks alongside activation of intrinsic cell death pathways. Its selectivity toward malignant cells, combined with a mechanistically validated mode of action, indicates strong potential for development as a standalone or adjuvant therapeutic agent, particularly in HER2-positive tumors where resistance to existing therapies remains a significant clinical challenge.

This study is limited to in vitro models; the in vivo efficacy, pharmacokinetics, bioavailability, and long-term safety of tangeretin remain unaddressed. Additionally, its direct molecular interactions with HER2 or AKT require further mechanistic validation.

Conclusion

This study identifies tangeretin as a selective and potent anti-cancer agent against HER2-positive breast cancer, demonstrating strong cytotoxicity toward SKBR3 cells while sparing non-tumorigenic MCF-10A cells. Its efficacy is mediated through coordinated inhibition of the HER2–PI3K/AKT/mTOR survival pathway and activation of intrinsic mitochondrial apoptosis.

Financial Support

Self-funded

Ethical Issue

The guidelines about the development, acquisition, authentication, cryopreservation, and transfer of cell lines between laboratories were strictly followed. Besides, microbial contamination (commonly mycoplasma), characterization, instability, and misidentification was considered seriously

Conflict of Interest

Authors declare no conflict of interest

Acknowledgement

The authors express their sincere gratitude to Chaitanya Deemed to be University, Warangal–506001, for providing the research facilities, technical support, and necessary infrastructure required to carry out this work

References

Braga CP, Ferreira AK, Ribeiro DL, Da Silva PH, Chaves DS, São Pedro GM, Antunes LM. Tangeretin enhances doxorubicin-mediated cytotoxicity by modulating apoptosis. Phytomedicine 2021; 81: 153422.

Brix N, Samaga D, Hennel R, Gehr K, Rödel F, Zips D, Brüchner K. Establishment of clonogenic survival assays for radiobiological analysis of cancer cell lines *in vitro*. Radiat Oncol. 2020; 15: 37.

Chen J, Xu B, Sun J. Polymethoxylated flavones as modulators of oncogenic signaling in human cancers. Biomed Pharmacother. 2019; 112: 108682.

Chen J, Xu J, Yu H. Anticancer activities of polymethoxylated flavones from citrus. J Funct Foods. 2020; 64: 103708.

Crowley LC, Christensen ME, Waterhouse NJ. Measuring cell death by microscopy and flow cytometry. Methods Mol Biol. 2016; 1419: 65-75.

Fang CY, Lin YW, Wu CL, Hou WC, Chou YC, Chen YK. Tangeretin suppresses PI3K/AKT signaling and inhibits tumor growth. Cancer Lett. 2016; 370: 265-73.

Guo S, Sun Y, Wang Y. Pharmacological properties of tangeretin. Food Funct. 2014; 5: 2392-400.

Huang CY, Chiang SF, Lin TY. Targeting PI3K/AKT signaling in breast cancer: Molecular mechanisms and therapeutic perspectives. Cancer Lett. 2018; 420: 1-9.

Lai CS, Ho CT, Pan MH. Polymethoxylated flavones activate apoptotic pathways and inhibit carcinogenesis. Mol Nutr Food Res. 2011; 55: 32-45.

Lai CS, Wu JC, Pan MH. Tangeretin inhibits breast cancer cell proliferation and enhances paclitaxel sensitivity. Cancer Lett. 2007; 251: 158-70.

Lee MH, Kim JH. Flavonoid-induced modulation of PI3K/AKT/mTOR pathway in breast cancer cells. Mol Carcinog. 2020; 59: 324–39.

Li Y, Ding X, Li Y, He S. Tangeretin: Chemistry, pharmacological properties, and potential applications. Front Pharmacol. 2022; 13: 864112.

Liu K, Liu P. Dual AO/EB staining to detect apoptosis in osteosarcoma cells. Med Sci Monit Basic Res. 2015; 21: 15-24.

Loibl S, Gianni L. HER2-positive breast cancer. Lancet 2017; 389: 2415-29.

Loibl S, Majewski I, Guarneri V, Nekljudova V, Holmes E, Bria E, Denkert C, Schneeweiss A, Schem C, Sotiriou C, Andre F, Conte P, Fasching PA, Hurvitz S, Carey LA, Colleoni M, Krop I, Baselga J. PIK3CA mutations and survival in operable breast cancer. J Clin Oncol. 2016; 34: 123-31.

Maadi H, Kazemi T, Ghasemi A, Asgarian-Omran H, Shabani M, Sharifian R, Mehrzad J. IP-kinase assay: A non-radioactive method to assess kinase activity. Bio-protocol 2014; 4: e1059.

Mayer IA, Arteaga CL. The PI3K/AKT pathway as a target for cancer treatment. Clin Cancer Res. 2016; 22: 2550-57.

Miller TW, Rexer BN, Garrett JT, Arteaga CL. Mutations in the phosphatidylinositol 3-kinase pathway: Role in tumor progression and therapeutic resistance. Cancer Res. 2011; 71: 560-65.

Miyata Y, Matsuo T, Sagara Y, Fujii T, Okada K, Ohba K, Sakai H. Antitumor properties of polymethoxylated flavones. Biofactors 2018; 44: 303-12.

Moja L, Tagliabue L, Balduzzi S, Parmelli E, Pistotti V, Guarneri V, D Amico R. Trastuzumab-containing regimens for early breast cancer. Cochrane Database Syst Rev. 2012; CD006243.

Niles AL, Moravec RA, Riss TL. Caspase-Glo® assays for apop -tosis research. Assay Guidance Manual. Bethesda (MD): Eli Lilly & NCBI, 2016; pp 1-24.

Panche AN, Diwan AD, Chandra SR. Flavonoids: An overview. J Nutr Sci. 2016; 5: e47.

Park JY, Kim EN, Kim JS. Flavonoid-mediated checkpoint activation leads to G2/M arrest in breast cancer cells. Oncol Rep. 2016; 35: 876-84.

Pozarowski P, Darzynkiewicz Z. Analysis of cell cycle by flow cytometry. Methods Mol Biol. 2004; 281: 301-12.

Rimawi MF, Schiff R, Osborne CK. Targeting HER2 for the treatment of breast cancer. Annu Rev Med. 2015; 66: 111-28.

Riss TL, Moravec RA, Niles AL, Benink HA, Worzella TJ, Minor L. Cell viability assays. Assay Guidance Manual. Bethesda (MD): Eli Lilly & NCBI, 2016.

Schneider CA, Rasband WS, Eliceiri KW. NIH Image to ImageJ: 25 years of image analysis. Nat Methods. 2012; 9: 671-75.

Singh A, Sharma R, Mehra R. HER2-driven signaling and resistance in breast cancer: Therapeutic implications. Front Oncol. 2021; 11: 651233.

Slamon DJ, Leyland-Jones B, Shak S, Fuchs H, Paton V, Bajamonde A, Fleming T, Eiermann W, Wolter J, Pegram M, Baselga J, Norton L. Use of chemotherapy plus a monoclonal antibody against HER2 for metastatic breast cancer that overexpresses HER2. N Engl J Med. 2001; 344: 783-92.

Sung H, Ferlay J, Siegel RL, Laversanne M, Soerjomataram I, Jemal A, Bray F. Global cancer statistics 2020: GLOBOCAN estimates of incidence and mortality worldwide for 36 cancers in 185 countries. CA Cancer J Clin. 2021; 71: 209-49.

Vu T, Claret FX. Trastuzumab resistance: Mechanisms and clinical implications. Breast Cancer Res. 2012; 14: 203.

Wang X, Zhang H, Chen L. Differential responsiveness of ER-positive breast cancer cells to natural flavonoids. J Cell Biochem. 2017; 118: 3834-45.

Zhang L, Xu J, Zhang Y, Wang Y. Tangeretin reverses multidrug resistance in breast cancer cells. J Cell Biochem. 2020; 121: 1557-69.

Zhao Y, Chen X, Li L. DNA fragmentation patterns during apoptosis: Evidence and techniques. Cell Death Dis. 2019; 10: 750.

Zhao Y, Chen X, Li L. Flavonoid-induced mitochondrial dysfunction in cancer apoptosis. Cell Death Dis. 2020; 11: 193.

Author Info

Puligilla Shankaraiah (Principal contact)
e-mail: drspuligilla.cu@outlook.com